A Unified Analytical Model and Experimental Validations of Injection-Locking Processes

Harris P. Moyer and Afshin S. Daryoush, *Fellow, IEEE*

***Abstract*—Unified analytical expressions predicting the locking range for fundamental, subharmonic ($n = 2$), superharmonic ($n = 2$), and parametric injection ($m = n = p = 1$) locking are presented and compared in this paper. Power series are employed to model the device nonlinearity. The a-parameters, relating nonlinear *I–V* behavior, are extracted using a harmonic-balance approach. These expressions are verified using an UHF oscillator; and good agreement is obtained between the experimental and analytical results.**

***Index Terms*—Harmonic balance, injection locking, microwave oscillator, nonlinear circuits, parametric injection locking, power series.**

I. Introduction

STABILIZED oscillators, employed for frequency translations, are an important front-end part in any electronics systems. One method of oscillator stabilization, made popular in the 1950's and 1960's, is injection locking [1], [2]. This technique involves injecting a stable reference signal into a free-running oscillator. Injection-locking methods are now becoming popular once again in a variety of applications [3]–[5].

Different methods of injection locking are reported [1], [2], [6]–[9]. Fundamental locking [1], [2] occurs when $f_{\rm inj} \approx f_{\rm lo}$; a large associated locking range is obtained, however, a stable source at a frequency close to the frequency of oscillation must be available. When $f_{\rm inj} \approx f_{\rm lo}/n$, an nth subharmonic injection locking [6] takes place with a reduced locking range. Superharmonic injection locking [7] is observed when $f_{\rm inj} \approx nf_{\rm lo}$, however, this technique has not been fully investigated due to difficulty of having a stable injection source at a frequency many times the free-running oscillator. Parametric injection locking [8] has also not received much attention since it occurs when $mf_{\rm inj1} + nf_{\rm inj2} \approx pf_{\rm lo}$, requiring two injection sources. The idler method [9] is the same as the parametric only when one source is replaced with a high-Q idler; i.e., $mf_{\rm inj1} + nf_{\rm idler} \approx pf_{\rm lo}$. The mixing of the injected signal with a local oscillator generates a sideband, which is passed through a high-Q filter and fed back into the oscillator along with the injected signal. A single source is used in this "pseudo" parametric approach. However, a high-Q idler is required at a frequency close to the oscillator frequency. Thus, the idler approach has not been extensively pursued.

Manuscript received August 18, 1998.

H. P. Moyer is with Hughes Space and Communications, El Segundo, CA 90245 USA.

A. S. Daryoush is with the Microwave Photonics Computer-Aided Design Laboratory, Department of Electrical and Computer Engineering, Drexel University, Philadelphia, PA 19104 USA.

Publisher Item Identifier S 0018-9480(00)02786-1.

Most of the reported analytical models for the injection-locked oscillators are based on the quasi-linear solution of differential equations in one-port circuits [1], [2]. However, the reported results in the literature do not model the different locking processes using a unified approach. A unified analytical model needs to be developed to compare merits of various injection-locking methods. With the advent of transistors and their popularity over diodes, injection-locking range calculations should be presented for two-port networks. The purpose of this paper is to present a unified modeling of injection-locked oscillators that are based on two-port network models. Therefore, analytical results comparing the various injection-locking methods are presented for a feedback-based oscillator. The analytical models are then experimentally verified and conclusions are drawn.

II. Background

The initial analytical modeling of the injection-locked oscillators are reported by Adler [1] and Kurokawa [2]. To extend their analyses to the case of a two-port network, nonlinear analysis methods such as a power series, Volterra series, or the harmonic balance could be applied to compare the locking ranges for the various injection-locking techniques.

A power series is a possible method for characterizing the perturbation of an oscillating system resulting from an injected signal. Traditionally, power series have been utilized to characterize mild nonlinearities in amplifiers [10]. Oscillator analysis is more difficult for two reasons. The first is that the power series cannot handle the dynamic nonlinearity associated with the input capacitance of a transistor. Thus, the oscillation condition may not be accurately determined. The second reason is that if the power series representation could account for the device memory, a large number of terms would be required to model the full operating range of the transistor.

A Volterra series is able to account for dynamic nonlinearities, but becomes difficult to apply when the nonlinearity is large. Previously, Volterra series have been used to model systems with mutiple inputs and a mild nonlinearity, such as would be found in a receiver front-end [11], even though attempts are made recently to apply that to strongly nonlinear systems such as self-oscillating mixers [12]. The harmonic-balance method using a full nonlinear transistor model such as the Gummel–Poon [13] or Curtice [14] has only been recently applied to injection locking [15]. As this method matures, it will be able to predict the locking range under a specific excitation, but will not indicate how each of the different methods will perform relative to each other.

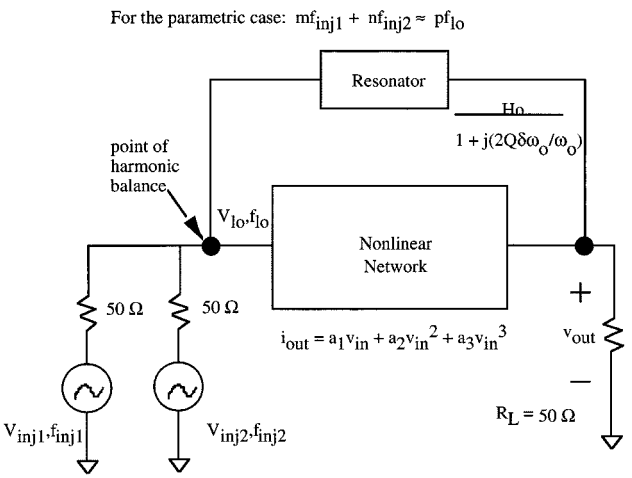

Fig. 1. Diagram of system to be analyzed for basic parametric injection locking. Removing one of the sources allows for the analysis of fundamental, subharmonic, and superharmonic injection locking.

The best method of developing an analytical model for injection combines the power series and harmonic-balance method [6]. The oscillation condition is determined from a full nonlinear model, which determines the operating point of the device. This procedure may be done using a harmonic-balance simulator such as Microwave Harmonica[1] or a time-domain simulator similar to the transient time-domain test bench in Libra.[2] Once the operating point has been determined, the series is applied to determine the nature of the nonlinearity at this point. Thus, the number of terms retained depends on the amount of perturbation one expects about the operating point.

III. Analytical Modeling

The first step in developing a universal set of locking-range equations is to define the oscillator system to be analyzed. Fig. 1 depicts a basic feedback oscillator with two injection sources to be used for the case of parametric injection locking. Removing one of the sources allows for analysis of fundamental, subharmonic, and superharmonic injection locking. The system consists of a single pole in parallel with a nonlinear gain element. A power series describes the nonlinear voltage–current relationship, and the injected voltage provides a stable reference at the input of the nonlinear element.

The oscillator has reached the steady-state voltage of $v_{\rm lo}$ at the input of the nonlinear device before the stable source is injected. The injected voltage of $v_{\rm inj}$ now perturbs this input voltage. The harmonic-balance method is applied to determine the change in the oscillator-input voltage and the associated locking range. Derivation of the locking-range equation in the case of parametric injection locking is presented since it has not been reported. The analyses for the fundamental, subharmonic ($n = 2$), and superharmonic ($n = 2$) follow the same procedure.

Currently, basic parametric locking (i.e., $m = 1$, $n = 1$, $p = 1$ in Fig. 1) is the only realistic type of forced oscillation that could be implemented in weakly nonlinear circuits.

[1]Microwave Harmonica is a Trademark of Ansoft Software, Inc., Pittsburgh, PA.

[2]Libra is a Trademark of Agilent EEsof, Westlake Village, CA.

The difficulty in implementing higher order parametric injection locking arises from the inefficient generation of higher order mixing products. This situation allows for an accurate solution to be obtained using the first three terms of the power series to model the nonlinearity. Fig. 1 indicates that the point of the harmonic balance is to occur at the input of the nonlinear network.

The first step is to define the input voltage to the nonlinear network $v_{\rm lo}$ and the injection voltages $v_{\rm inf}$ and $v_{\rm inj2}$

$$V_{\rm lo} = \frac{V_{\rm lo}}{2} \cdot \left[e^{j\omega_{\rm lo}t} + e^{-j\omega_{\rm lo}t}\right] \tag{1}$$

$$V_{\rm inj1} = \frac{V_{\rm inf1}}{2} \cdot \left[e^{j(\omega_{\rm inj1}t+\phi_1)} + e^{-j(\omega_{\rm inj1}t+\phi_1)}\right] \tag{2}$$

$$v_{\rm inj2} = \frac{v_{\rm inj2}}{2} \cdot \left[e^{j(\omega_{\rm inj2}t+\phi_2)} + e^{-j(\omega_{\rm inj2}t+\phi_2)}\right]. \tag{3}$$

These voltage components are mixed together in the nonlinear network and fed back through the bandpass ($\omega_o = \omega_{\rm lo}$) resonator to the input node to balance all the harmonics. The mixing process may be defined as an output current in terms of the nonlinear transconductance

$$i_{\rm out} = \sum_{n=1}^{\infty} a_n v^n \tag{4}$$

$$\begin{aligned} i_{\rm out} \cong\, & a_1(v_{\rm lo} + v_{\rm inj1} + v_{\rm inj2}) + a_2(v_{\rm lo} + v_{\rm inj1} + v_{\rm inj2})^2 \\ & + a_3(v_{\rm lo} + v_{\rm inj1} + v_{\rm inj2})^3. \end{aligned} \tag{5}$$

From many terms generated as a result of expansion in (5), the terms of interest are those that fall close to $f_{\rm lo}$. The following components at $f_{\rm lo}$ are generated:

$$\text{From } a_1v_{\rm in} \rightarrow A_1\,\frac{v_{\rm lo}}{2}\,e^{j\omega_{\rm lo}t}$$

$$\text{From } a_2v_{\rm in}^2 \rightarrow a_2 \cdot \left(\frac{v_{\rm inj1}v_{\rm inj2}}{2}\right) \cdot e^{j((\omega_{\rm inj1}+\omega_{\rm inj2})t+(\phi_1+\phi_2))}$$

$$\text{From } a_3v_{\rm in}^3 \rightarrow 3a_3 \cdot \left[\left(\frac{v_{\rm lo}}{2}\right)^3 + \left(\frac{v_{\rm lo}v_{\rm inj1}^2}{4}\right) + \left(\frac{v_{\rm lo}v_{\rm inj2}^2}{4}\right)\right] \cdot e^{j\omega_{\rm lo}t}.$$

In these expressions, the conjugate term has been dropped to simplify the analysis.

Next, these components must be passed through the resonator back to the input for the harmonic balance to be performed. In equilibrium, the voltage at $f_{\rm lo}$ fed through the resonator must be equal to $v_{\rm lo}$, which is the input to the amplifier at $f_{\rm lo}$. The harmonic balance of $f_{\rm lo}$ at the input node results in

$$\begin{aligned} & \frac{R_L \cdot H_o}{1 + j\left(\dfrac{2Q\delta\omega}{\omega}\right)} \\ & \quad \cdot \left\{ a_1\,\frac{v_{\rm lo}}{2} + a_2\left(\frac{v_{\rm inj1}v_{\rm inj2}}{2}\right) \cdot e^{j(\phi_1+\phi_2)} \right. \\ & \quad \left. + 3a_3\left[\left(\frac{v_{\rm lo}}{2}\right)^3 + \left(\frac{v_{\rm lo}v_{\rm inj1}^2}{4}\right) + \left(\frac{v_{\rm lo}v_{\rm inj2}^2}{4}\right)\right]\right\} \\ & = \frac{v_{\rm lo}}{2}. \end{aligned} \tag{6}$$

The R_L term is the load resistance. Equation (6) is now expanded into its real and imaginary parts by multiplying the top and bottom of the left-hand side of the equation by the quantity $[1 - j(2Q\delta\omega_o/\omega_o)]$. The resulting equations for the real and imaginary are as follows.

Real Part:

$$\frac{R_L \cdot H_o}{1+\left(\frac{2Q\delta\omega}{\omega}\right)^2} \cdot \left[a_1 \frac{v_{\rm lo}}{2} + a_2\left(\frac{v_{\rm inj1}v_{\rm inj2}}{2}\right) \cdot \left(\cos(\phi_1+\phi_2)+\sin(\phi_1+\phi_2)\cdot\left(\frac{2Q\delta\omega}{\omega}\right)\right) + 3a_3\left[\left|\frac{v_{\rm lo}}{2}\right)^3 + \left(\left|\frac{v_{\rm lo}v_{\rm inj1}^2}{4}\right| + \left(\frac{v_{\rm lo}v_{\rm inj2}^2}{4}\right)\right]\right] = \frac{v_{\rm lo}}{2}. \tag{7}$$

Imaginary Part:

$$\frac{R_L \cdot H_o}{1+\left(\frac{2Q\delta\omega}{\omega}\right)^2} \cdot \left[a_1 \frac{v_{\rm lo}}{2}\cdot\left(\frac{-2Q\delta\omega}{\omega}\right) + a_2\left(\frac{v_{\rm inj1}v_{\rm inj2}}{2}\right) \cdot \left(\sin(\phi_1+\phi_2)-\cos(\phi_1+\phi_2)\cdot\left(\frac{2Q\delta\omega}{\omega}\right)\right)\right] + \frac{R_L \cdot H_o}{1+\left(\frac{2Q\delta\omega}{\omega}\right)^2}\cdot 3a_3\left[\left(\frac{v_{\rm lo}}{2}\right)^3 + \left(\frac{v_{\rm lo}v_{\rm inj1}^2}{4}\right) + \left(\frac{v_{\rm lo}v_{\rm inj2}^2}{4}\right)\right]\cdot\left(\frac{-2Q\delta\omega}{\omega}\right) = 0. \tag{8}$$

The real and imaginary equations may be solved simultaneously to obtain the output level of the oscillator $v_{\rm lo}$, and the locking range $\delta\omega_o$. Using the equation for the imaginary, the maximum normalized locking range may be solved for in terms of the injected voltage by setting the sum of the angles $\phi_1+\phi_2 = \pm 90°$. Doing this eliminates the cosine term and sets the sine term equal to one. The $\delta\omega_o$ term in the resulting equation is the maximum one-sided locking range for a given pair of injected voltages

$$\left(\frac{2Q\delta\omega}{\omega}\right) \cdot \left[a_1\frac{v_{\rm lo}}{2} + 3a_3\left[\left(\frac{v_{\rm lo}}{2}\right)^3 + \left(\frac{v_{\rm lo}v_{\rm inj1}^2}{4}\right)\left(\frac{v_{\rm lo}v_{\rm inj2}^2}{4}\right)\right]\right] = a_2\left(\frac{v_{\rm inj1}v_{\rm inj2}}{2}\right). \tag{9}$$

TABLE I
CHART COMPARING THE ANALYTICAL EXPRESSIONS FOR THE LOCKING RANGE ASSOCIATED WITH DIFFERENT TYPES OF INJECTION LOCKING

Injection Locking Method	Normalized Locking Range
Fundamental $f_{\rm lo} \approx f_{\rm inj}$	$\frac{a_1\frac{v_{\rm inj}}{2} + a_3\left[3*\left(\frac{v_{\rm lo}}{2}\right)^3 + \frac{v_{\rm inj}^2 v_{\rm lo}}{8} + 3*\frac{v_{\rm lo}^2 v_{\rm inj}}{8}\right]}{a_1\frac{v_{\rm lo}}{2} + a_3\left[3*\left(\frac{v_{\rm lo}}{2}\right)^3 + 5*\frac{v_{\rm inj}^2 v_{\rm lo}}{8}\right]}$ (11)
2nd Subharmonic [6] $f_{\rm inj} \approx f_{\rm lo}/2$	$\frac{a_2\left(\frac{v_{\rm inj}^2}{4}\right)}{a_1\frac{v_{\rm lo}}{2} + 3a_3\left[\left(\frac{v_{\rm lo}}{2}\right)^3 + \left(\frac{v_{\rm lo}v_{\rm inj}^2}{4}\right)\right]}$ (12)
2nd Superharmonic $f_{\rm inj} \approx 2f_{\rm lo}$	$\frac{a_2\left(\frac{v_{\rm lo}v_{\rm inj}}{2}\right)}{a_1\frac{v_{\rm lo}}{2} + 3a_3\left[\left(\frac{v_{\rm lo}}{2}\right)^3 + \left(\frac{v_{\rm lo}v_{\rm inj}^2}{4}\right)\right]}$ (13)
Parametric $f_{\rm inj1} + f_{\rm inj2} \approx f_{\rm lo}$	$\frac{a_2\left(\frac{v_{\rm inj1}v_{\rm inj2}}{2}\right)}{a_1\frac{v_{\rm lo}}{2} + 3a_3\left[\left(\frac{v_{\rm lo}}{2}\right)^3 + \left(\frac{v_{\rm lo}v_{\rm inj1}^2}{4}\right) + \left(\frac{v_{\rm lo}v_{\rm inj2}^2}{4}\right)\right]}$ (10)

Solving for the normalized locking range yields

$$\frac{2Q\delta\omega}{\omega} = \frac{a_2\left(\frac{v_{\rm inj1}v_{\rm inj2}}{2}\right)}{a_1\frac{v_{\rm lo}}{2} + 3a_3\left[\left(\frac{v_{\rm lo}}{2}\right)^3 + \left(\frac{v_{\rm lo}v_{\rm inj1}^2}{4}\right) + \left(\frac{v_{\rm lo}v_{\rm inj2}^2}{4}\right)\right]}. \tag{10}$$

This equation defines the normalized locking range for basic parametric injection locking using a three-term series. A summary of the results for the fundamental, basic parametric, subharmonic ($n = 2$), and superharmonic ($n = 2$) is presented in Table I. These locking range equations (i.e., (10) and [Table I, eq. (11)–(13)]) allow for comparison of various injection-locking methods in a specific oscillator.

IV. EXPERIMENTAL VALIDATION

To verify the derived injection-locking range (i.e., (10) and (11)–(13) in Table I) that are shown in Table I, experiments are conducted for a feedback oscillator. The UHF oscillator is realized using a bipolar junction transistor (BJT) (Siemens BFP405) and replicates the system block diagram shown in Fig. 1. The quality Q-factor of the oscillator may be predicted by the following equation describing the bandpass resonator:

$$S_{21}(\text{dB}) = \frac{-27.3 f_o \tau}{Q_u} \tag{14}$$

where f_o is the resonant frequency, τ is the resonantor's group delay, and Q_u is the unloaded Q-factor. From network analyzer measurements ($|S_{21}| \approx -12.5$ dB, $f_o \approx 770$ MHz, and $\tau \approx 3.84$ ns), a Q_u of 6.45 is calculated for the feedback circuit.

Gummel–Poon model parameters of the BJT, provided by the manufacturer, are employed for SPICE modeling. Nonlinear simulation of the oscillator is conducted using the MWSPICE model in the time-domain bench of Libra. The simulated oscillation frequency is 770.5 MHz with an output power of -5 dBm; the measured results are output power of -3.8 dBm at $f_{\rm lo} \approx 740$ MHz. Since the oscillator is modeled accurately, then the simulation technique may be used to extract the a-parameters of the gain block, which are important parameters in the locking-range equations.

The method of a-parameter extraction is presented in Appendix. Results from the extraction may be summarized as follow [cf. (A.1)–(A.3)]: $a_1 = 0.05475\angle 102.96°$S, $a_2 = 0.11823\angle -103.2°$S/V, and $a_3 = 0.629\angle -50.45°$S/V^2. These a-parameter values are valid for the simulated oscillator operating condition and may be used in (10) and (11)–(13) in Table I. The locking ranges for the different injection-locking methods are measured and compared with predicted results for the feedback oscillator.

The experimental verification of the derived equations are now presented. The experimental setup consists of a Rohde–Schwarz (100 kHz–1 GHz) signal generator and a Systron Donner (model #1626) microwave synthesizer used as injection sources and a Tektronix (2756P) spectrum analyzer to measure the power spectra. The injected power levels are limited to 15 dB below the oscillator's output power so that a weakly nonlinear assumption remains valid. The minimum injected power level is also selected by the frequency resolution the injected synthesized source and the oscillator frequency drift. The oscillator drift is as result of temperature and loading of the circuit.

The first step is to measure the fundamental locking range to verify the $Q_{\rm ext}$ of the oscillator. The fundamental injection-locking range may be reduced to an expression similar to the Adler's locking range [1] by neglecting the small effects of higher order terms in (11) (see Table I). The derived equation is

$$\Delta\omega_o = \frac{\omega_o}{2Q_{\rm ext}} \cdot \frac{V_{\rm inj}}{V_{\rm out}}. \tag{15}$$

By fitting the experimental data for fundamental injection locking, a $Q_{\rm ext}$ of six is calculated. This predicted result is close to $Q_u \approx 6.45$, the predicted unloaded Q of the bandpass resonator.

This Q value is applied to the normalized locking range equations for subharmonic ($n = 2$), superharmonic ($n = 2$), and parametric ($m = 1, n = 1, p = 1$). Figs. 2 and 3 depict the locking range ($\Delta\omega_o$) as a function of the injected power gain ($P_{\rm inj}/P_{\rm out}$) of the second subharmonic and superharmonic cases (i.e., $n = 2$). The experimental and analytical results match; the difference is, at worst, a factor of two. Fig. 4(a)–(c) presents parametric injection-locking range as a function of the injected power gain. The locking range is measured as two

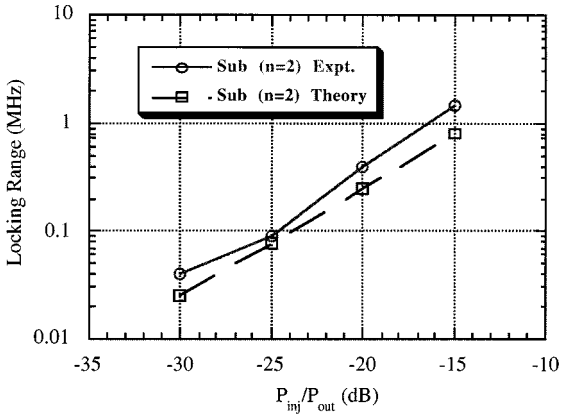

Fig. 2. Plot of the subharmonic ($n = 2$) locking range as a function of injected power gain ($P_{\rm inj}/P_{\rm out}$) comparing the experimental and analytical results.

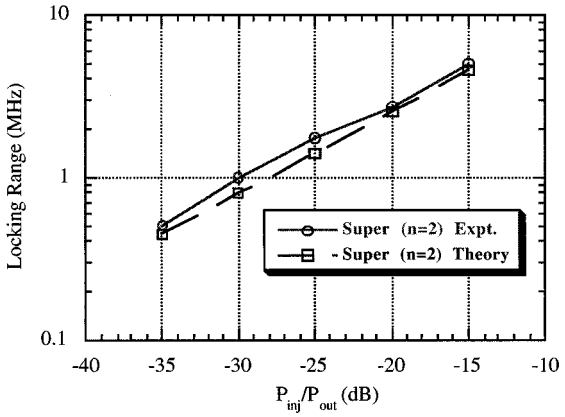

Fig. 3. Plot of the superharmonic ($n = 2$) locking range as a function of injected power gain ($P_{\rm inj}/P_{\rm out}$) comparing the experimental and analytical results.

sources with equal input powers, however, different frequencies are injected to the UHF oscillator.

The predicted and measured parametric injection-locking range results are in relative good agreement. As the frequency difference becomes more pronounced (i.e, $f_{\rm inj1} = 610$ MHz and $f_{\rm inj2} = 130$ MHz), the match between experimental and theoretical results degrades. The case when unequal power levels are injected shows the same trend of frequency-dependent behavior. Table II depicts locking range when the power levels are off by 5 dB. These results indicate that the greater the frequency difference, the greater the effect of the offset power. The case of 130–610 MHz (the 130-MHz signal being 5 dB lower than the 610-MHz signal) and 610–130 MHz shows more disparity than both of the other frequency combinations.

V. Discussion

Using the fundamental data as a baseline, the analytical model compares well with the experimental. For the parametric injection-locking cases, there is a frequency dependence more pronounced than with the $n = 2$ subharmonic or superharmonic cases. Even with this frequency dependence, the results still fall within a factor of three in the worst case. This degradation may

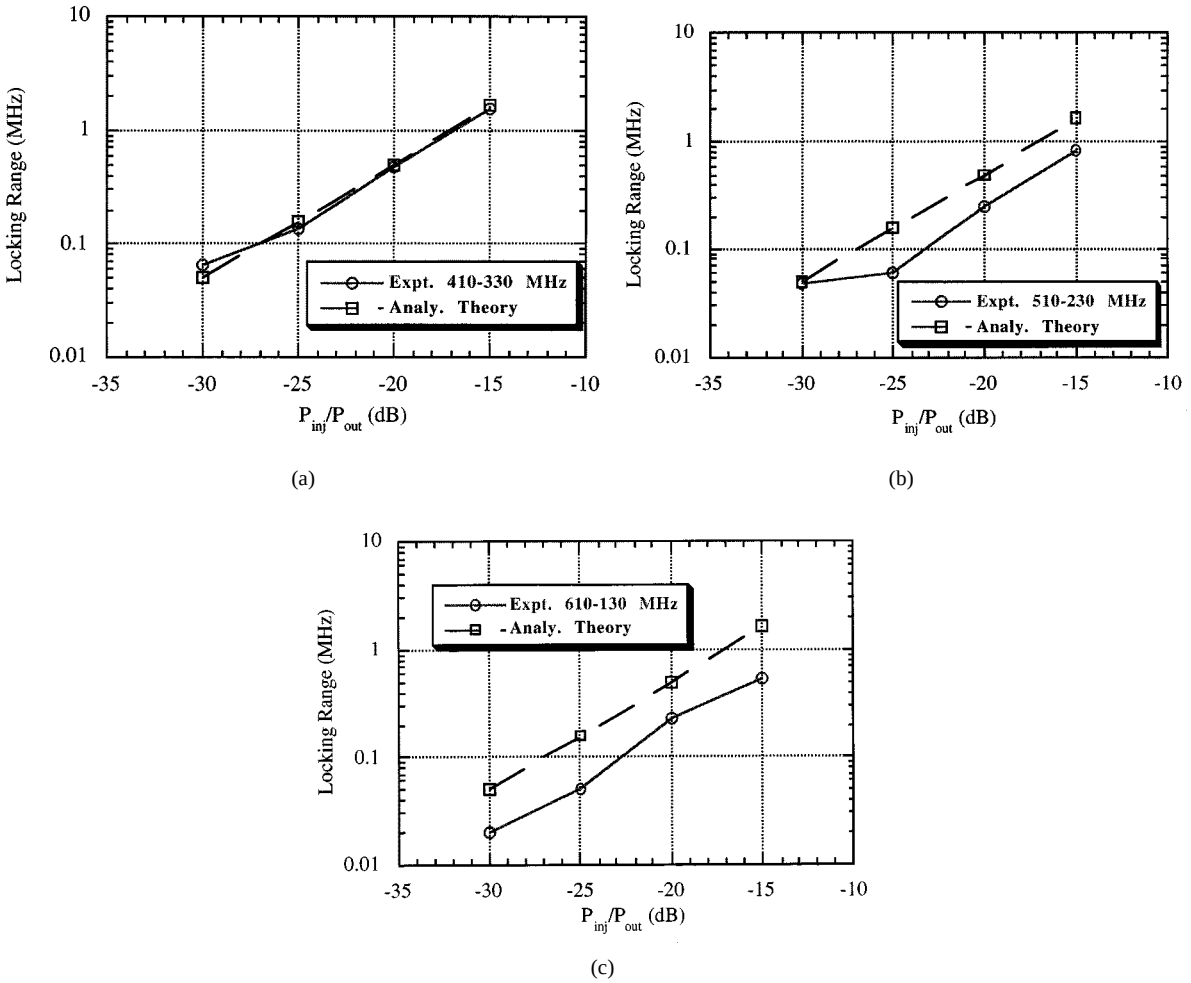

Fig. 4. Parametric injection-locking range as a function of injected power gain ($P_{\rm inj}/P_{\rm out}$) with equal input powers. (a) Frequencies of 410 and 330 MHz, (b) 510 and 230 MHz, and (c) 610 and 130 MHz.

be explained by the frequency dependence of the a-parameters as the frequency is varied over a wide range.

Comparing the measured locking ranges, one can see that the superharmonic provides the largest locking range and that the parametric locking range (assuming equal power levels) is greater than the subharmonic. For equal injection levels, (10) indicates that the parametric locking range should ideally be twice as high as the subharmonic locking range defined by (12) in Table I. However the measurements indicates that this factor is between 1.2–1.5 times higher. One interesting result is the large superharmonic injection-locking range. The locking range is 3–4 times higher than the corresponding $n = 2$ subharmonic injection locking. A higher value should be expected since (13) in Table I indicates that the locking range is proportional to $v_{\rm lo} \cdot v_{\rm inj}$ instead of $v_{\rm inj}^2$, even though Forrest *et al.* [7] proposed superharmonic injection locking as a means of phase shifting in antenna arrays, but does not indicate this distinct advantage of superharmonic injection locking over the subharmonic injection locking.

Although the analytical model does well at predicting the locking range for low-to-intermediate injected power levels, it does not describe the properties of the process. Properties of injection locking such as the locked output power, asymmetric locking ranges, and Type-II injection locking cannot be predicted. Possible methods to predict these attributes are time-domain simulations transformed to the frequency domain [16] or a full harmonic-balance routine, as demonstrated by Rizzoli *et al.* [15].

VI. Conclusion

For the first time, unified equations have been presented, predicting the injection-locking range of fundamental, subharmonic ($n = 2$), superharmonic ($n = 2$), and parametric ($m = 1$, $n = 1$) injection-locked two-port oscillators. These equations are applicable to oscillators constructed with transistors (two-port devices) and provide a method of comparison between the different methods for a specific oscillator. Using these equations, merit of each injection-locking techniques could now be analytically compared depending on the forced oscillation application and the free-running oscillator topology.

Experimental results indicate good agreement with the theory. Including in the extracted a-parameters frequency dependence in addition to its level dependence could make further model improvement. The derived analytical results could also be expanded to the higher order injection-locking

TABLE II
CHARTS COMPARING THE LOCKING RANGES FOR PARAMETRIC INJECTION LOCKING WITH UNEQUAL POWER LEVELS BEING INJECTED FOR: (a) 330 AND 410 MHz, (b) 230 AND 510 MHz, AND (c) 130 AND 610 MHz. THE LOWER POWER LEVEL IS ATTRIBUTED TO THE FIRST FREQUENCY INDICATED AT THE HEAD OF THE COLUMN

P_{inj1}/P_{inj2} (dBm)	Theory	330-410 MHz	410-330 MHz
-30/-25	88 KHz	85 KHz	85 KHz
-25/-20	280 KHz	240 KHz	235 KHz
-20/-15	900 KHz	1005 KHz	895 KHz

(a)

P_{inj1}/P_{inj2} (dBm)	Theory	230-510 MHz	510-230 MHz
-30/-25	88 KHz	50 KHz	45 KHz
-25/-20	280 KHz	110 KHz	115 KHz
-20/-15	900 KHz	310 KHz	385 KHz

(b)

P_{inj1}/P_{inj2} (dBm)	Theory	130-610 MHz	610-130 MHz
-30/-25	88 KHz	35 KHz	55 KHz
-25/-20	280 KHz	110 KHz	145 KHz
-20/-15	900 KHz	275 KHz	465 KHz

(c)

processes, though not practical in weakly nonlinear systems. Note that the injection locking of oscillators could also be extended to its optical counterparts [17].

APPENDIX

DERIVATION OF THE a-PARAMETERS FOR THE GAIN BLOCK

Level-dependent nonlinear a-parameters are used to characterize the nonlinear current–voltage relationship in the gain block of the oscillator. To accurately simulate the BJT-based amplifier behavior, the Gummel–Poon model [13] provided by the manufacturer is used. This appendix describes how to extract the nonlinear a-parameters at a particular frequency and power level. The basis of the extraction is a time domain simulation in Libra, which is used to determine the input voltage to the transistor under the oscillation condition. The parameters are determined from the output current that is a nonlinear function of the input voltage.

For extracting the a-parameters of the BJT, the first step is to use the time-domain simulator to determine the base voltage under the oscillation condition. Once this voltage has been determined, an equivalent source voltage (in a 50-Ω system) at the frequency of oscillation is employed to recreate this voltage on the base. The next step is to simulate the device as an amplifier in a 50-Ω system with the same bias condition: the base voltage set to 2.4 V and the collector voltage set to 3.0 V, which produces a collector current of 5 mA. The resulting power spectrum

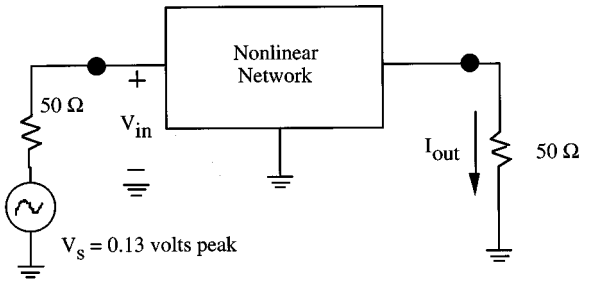

Fig. 5. Diagram of the amplifier used to determine the a-parameters. The source is set to give an input voltage of 0.09-V peak.

contains the fundamental signal, set at 750 MHz, and its harmonics. Fig. 5 shows the transition from the oscillator (cf. Fig. 1) to an amplifier with an equivalent voltage amplitude at the base.

From the time-domain test bench, the transistor base voltage in the oscillation condition is simulated to be $\approx$0.09-V peak. A generator with a 50-Ω source impedance must be driven at 0.13-V peak at an angle of 0° in the harmonic-balance test bench to generate 0.0637-V rms ($-$0.09-V peak) at the base of the transistor. The phase of the input voltage is $-35.95°$. The phase of the input voltage is accounted for when calculating the a-parameters.

The power spectra resulting from this excitation may be used to determine the output current at each harmonic frequency. The a-parameters are determined by dividing the harmonic currents by the input voltage

$$\begin{aligned} a_1 &= \frac{I_1(\omega_o}{v_{\text{in}}(\omega_o)} \\ &= \frac{3.49e^{-3}\angle 67.01}{0.0637\angle -35.9} \\ &= 0.054\,75\angle 102.96°\text{S} \end{aligned} \tag{A.1}$$

$$\begin{aligned} a_2 &= \frac{I_2(2\omega_o)}{V_{\text{in}}^2(\omega_o)} \\ &= \frac{4.8e^{-4}\angle -175.1}{(0.0637)^2\angle -71.9} \\ &= 0.118\,23\angle -103.2°\text{S/V} \end{aligned} \tag{A.2}$$

$$\begin{aligned} a_3 &= \frac{I_3(3\omega_o)}{V_{\text{in}}^3(\omega_o)} \\ &= \frac{1.63e^{-4}\angle -175.1}{(0.0637)^3\angle -107.86} \\ &= 0.629\angle -50.45°\text{S/V}^2. \end{aligned} \tag{A.3}$$

It is important to note that the a-parameters here are derived specifically for the simulated feedback oscillator. The calculated values are not necessarily valid if the oscillator's bias condition is changed in any manner. At microwave frequencies, the a-parameters will display more pronounced frequency dependence because of the device intrinsic and package parasitic.

REFERENCES

[1] R. Adler, "A study of locking phenomena in oscillations," *Proc. IRE*, vol. 34, pp. 351–357, 1946.

[2] K. Kurokawa, "Insection locking of microwave solid-state oscillators," *Proc. IEEE*, vol. 61, pp. 1386–1410, Oct. 1973.

[3] A. S. Daryoush, "Optical synchronization of millimeter-wave oscillators for distributed architectures," *IEEE Trans. Microwave Theory Tech.*, vol. 38, pp. 467–476, May 1990.

[4] J. Birkeland and T. Itoh, "A 16-element quasi-optical FET oscillator power-combining array with external injection locking," *IEEE Trans. Microwave Theory Tech.*, vol. 40, pp. 475–481, Mar. 1992.

[5] D. Wake *et al.*, "A 60-GHz 120-MB/s QPSK fiber-radio transmission experiment incorporating an electroabsorption modulator transceiver for a full duplex optical data path," in *IEEE MTT-S Int. Microwave Symp. Dig.*, vol. 1, Denver, CO, June 1997, pp. 39–42.

[6] X. Zhang, X. Zhou, and A. S. Daryoush, "A theoretical and experimental study of the noise behavior of subharmonically locked local oscillations," *IEEE Trans. Microwave Theory Tech.*, vol. 40, pp. 895–902, May 1992.

[7] A. Haq Al-Ani, A. L. Cullen, and J. R. Forrest, "A phase-locking method for beam steering in active array antennas," *IEEE Trans. Microwave Theory Tech.*, vol. MTT-22, pp. 698–703, June 1974.

[8] Y. Fukatsu and H. Kato, "Frequency conversion with gain through sideband locking of an IMPATT diode oscillation," *Proc. IEEE*, vol. 57, pp. 342–343, Mar. 1969.

[9] H. Okamoto and M. Ikeda, "Injection locking of an IMPATT diode oscillation by using a low-frequency signal parametric injection locking," in *IEEE MTT-S Int. Microwave Symp. Dig.*, San Diego, CA, 1977, pp. 234–236.

[10] S. A. Maas, *Nonlinear Microwave Circuits.* Norwood, MA: Artech House, 1988.

[11] J. J. Bussagang, L. Ehrman, and J. W. Graham, "Analysis of nonlinear systems with multiple inputs," *Proc. IEEE*, vol. 62, pp. 1088–1199, Aug. 1974.

[12] S. T. Chew and T. Itoh, "Application of Volterra series to the problem of self-oscillating mixer," *IEEE Trans. Microwave Theory Tech.*, vol. 44, pp. 269–274, Feb. 1996.

[13] H. K. Gummel and H. C. Poon, "An integral charge control model of bipolar transistors," *Bell Syst. Tech. J.*, vol. 49, pp. 827–851, 1970.

[14] W. R. Curtice and M. Ettenberg, "A nonlinear GaAs FET model for use in the design of output circuits for power amplifiers," *IEEE Trans. Microwave Theory Tech.*, vol. MTT-33, pp. 1383–1394, Dec. 1985.

[15] V. Rizzoli, A. Neri, and D. Masotti, "The application of harmonic-balance methodology to the analysis of injection locking," in *IEEE MTT-S Int. Microwave Symp. Dig.*, Albuquerque, NM, June 1992, pp. 1591–1594.

[16] H. P. Moyer, "Comparison of injection locking techniques using nonlinear methods," Ph.D. dissertation, Dept. Elect. Comput. Eng., Drexel Univ., Philadelphia, PA, June 1998.

[17] A. S. Daryoush, K. Sato, K. Horikawa, and H. Ogawa, "Electrically injection locked intermodal oscillation in a long optical cavity laser diode," *IEEE Microwave Guided Wave Lett.*, vol. 7, pp. 194–196, July 1997.

Harris P. Moyer was born in Madison, WI, in 1967. He received the B.S.E. degree in engineering physics from The University of Michigan at Ann Arbor, in 1989, the M.S.E.E. degree from the University of California at Santa Barbara, in 1993, and the Ph.D. degree from Drexel University, Philadelphia, PA, in 1998.

From 1990 to 1991, he was with Hughes Aircraft, Torrance, CA, where he worked on the design of microwave hybrid circuits and the testing and integration of monolithic-microwave integrated-circuit (MMIC) amplifiers. From 1996 to 1998, he was with Basic Commerce and Industries, Moorestown, NJ, where he developed high-power pulsed amplifiers and devices in conjunction with Lockheed Martin. He is currently with Hughes Space and Communications, El Segundo, CA, where he is involved with high-frequency packaging and MMIC design. He has authored or co-authored several papers on nonlinear microwave circuits. His areas of interest have included quasi-optical antenna elements, nonlinear modeling, oscillator stabilization techniques, and oscillator phase noise simulations.

Afshin S. Daryoush (S'84–M'86–SM'91–F'99) received the Ph.D. degree in electrical engineering from Drexel University, Philadelphia, PA, in 1986.

He then joined the faculty of Drexel University, as DuPont Assistant Professor of electrical and computer engineering, and in 1990, became an Associate Professor. During the summers of 1987 and 1988, he was a Summer Faculty Fellow at NASA-Lewis Research Center, Cleveland, OH, where he was involved with analog fiber-optic links for ACTS. In the summers of 1989 and 1990, he was with the Naval Air Development Center, Warminster, PA, as an ASEE Summer Faculty Fellow, where he was involved with low-power-consuming digital fiber-optic links, and was a Visiting Scholar at NTT Wireless Systems Laboratories, Yokosuka, Japan, from October 1996 to April 1997. He is currently with the Electrical and Computer Engineering Department, Drexel University. He has authored or co-authored over 150 technical publications, conducted research in microwave photonics, and lectured frequently at workshops and international symposia. He has served as guest editor for *The Journal of Franklin Institute* and *Microwave and Lightwave Technology Letters*.

Dr. Daryoush is a member of Sigma Xi and served as the Drexel University chapter chairman in 1997–1998. He has served in various capacities for the Philadelphia Joint Chapter of the IEEE Antennas and Propagation (IEEE AP-S) and IEEE Microwave Theory and Techniques Societies (IEEE MTT–S), including chairman from 1991 to 1993. He is the recipient of the Microwave Prize presented at the 16th European Microwave Conference, Dublin, Ireland, and has also received the 1986 Best Paper Award presented at the International Microwave Symposium, Baltimore, MD.